International Journal of Multiphase Flow 120 (2019) 103086

Contents lists available at ScienceDirect

International Journal of Multiphase Flow

journal homepage: www.elsevier.com/locate/ijmulflow

Statistical Moments Transport Model for the prediction of slug flow properties

J.R. Fagundes Netto[a], G.F.N. Gonçalves[a], A.P. Silva Freire[a,b,*]

[a] Núcleo Interdisciplinar de Dinâmica dos Fluidos(NIDF/UFRJ), Universidade Federal do Rio de Janeiro, Rua Moniz Aragão 360, Bloco 2, Rio de Janeiro 21941-972, Brazil

[b] Programa de Engenharia Mecânica (PEM/COPPE/UFRJ), Universidade Federal do Rio de Janeiro, C.P. 68503, Rio de Janeiro 21941-972, Brazil

ARTICLE INFO

Article history:
Received 12 April 2019
Revised 1 August 2019
Accepted 7 August 2019
Available online 8 August 2019

Keywords:
Statistical moments
Slug flow
Bubble distributions

ABSTRACT

The present work introduces the Statistical Moments Transport (SMT) Model for a description of the mean and standard deviation values of bubble and liquid slug lengths in horizontal, inclined and vertical flows. The model considers gas depressurization and the interaction (coalescence) between long bubbles. Results are compared to three other theoretical approaches – unit cell, slug tracking and slug capturing models – and six different experimental data sets. The gain in computing time as compared to the slug tracking model even in relatively short pipes is of two orders of magnitude.

1. Introduction

Horizontal slug flow has been a subject of major concern over the last 50 years. This is a very complex flow, characterized by alternated long bubbles and aerated liquid plugs traveling downstream. For the typical gas and liquid flow rates practiced in industry, information on the local flow conditions are impossible to obtain due to the very small time and length scales that would have to be resolved. Whereas for single phase flows resolving the small dissipative scales may be an option for low and moderate Reynolds numbers, multiphase flows pose the additional difficulty of correctly representing phase interfaces and their related phenomena.

Fortunately, to many problems of practical interest, predictions of volume (*or time*) averaged properties suffice to most design and operational requirements. As a natural consequence, the development of mechanistic and one-dimensional models based on the equations for mass, momentum and energy conservation has been diligently pursued by the scientific community. These models normally furnish data on liquid and gas fractions, pressure, velocities and temperatures and can be divided (*apud* Nydal, 2012) between those that "avoid small-scale phenomena" (e.g., unit cell models) and those that "resolve all scales" (e.g., capturing and tracking methods).

The purpose of the present work is to discuss a method that uses transport equations to obtain the statistical moments of bubble and liquid slug lengths. The length distributions of long bubbles (L_B) and liquid slugs (L_S) can be obtained from methods that resolve all flow scales, but these methods require a large computational time. The Statistical Moments Transport Model (SMT) furnishes data on the average values of L_B and L_S and their standard deviations, at a very modest computational time. The present formulation is compared to the unit cell model of Orell (2005), the slug tracking model of Cook and Behnia (2000), the slug capturing model of Evje and Flåtten (2003) and the experimental data introduced by Grenier (1997), Cook and Behnia (2000), Ujang et al. (2006), Mayor et al. (2008), Gonçalves et al. (2018) and van Hout et al. (2003).

In fact, most model formulations differ greatly in regard to their constitutive hypotheses and implementation details. Many different propositions can be easily identified for unit cell, slug tracking or slug capturing models. The above selection, nonetheless, offers a good representation of what is available in the literature for slug flow prediction.

To hamper misunderstandings on the implementation of the quoted models, their general premises and a few details are discussed in a specific section. The early models developed to predict the phase velocities and pressure gradient were based on the unit cell concept initially advanced by Wallis (1969). Dukler and Hubbard (1975) proposed the first comprehensive model. Shortly published subsequent papers strove on variations of the same concept. In, Fabre et al. (1989) proposed a different approach based on a statistical cell unit (see also Fabre and Liné, 1992). The developments just described quickly improved the ability of scientists and engineers to predict important flow parameters such

* Corresponding author.
E-mail addresses: gabrielfng@hotmail.com (G.F.N. Gonçalves), atila@mecanica.coppe.ufrj.br (A.P. Silva Freire).

https://doi.org/10.1016/j.ijmultiphaseflow.2019.103086
0301-9322/

as the pressure gradient, the mean phase velocities and the mean volume fractions. However, the same methods did not improve on the knowledge of the slug structure, i.e., very little advance was obtained on the prediction of the statistics of bubble and slug lengths and their evolution along a pipe.

Interesting early experimental works by Dhulesia et al. (1991), Nydal et al. (1992) and Grenier (1997), provided statistical descriptions on slug flows. Fagundes Netto (1999) studied the behavior of isolated bubbles in a liquid horizontal flow, focusing on the description of the bubble shape and the interaction between bubbles.

Possibly, the most popular approach to assess the evolution of the slug structure is the slug tracking method, where the volume and position of each individual bubble and slug are followed through the pipe length. The bubbles expand as pressure decreases and coalescence may occur. The flow structure is determined after a simulation time that ensures the passage, at any pipe position, of a large enough number of cells for a reliable statistical study. Grenier (1997), Nydal and Banerjee (1996), Barnea and Taitel (1993), Straume et al. (1992) and others applied this method to describe the slug structure evolution along a pipe. The present alternative approach, as mentioned before, uses transport equations for the statistical moments of bubble and liquid slug lengths. The present method takes into account gas depressurization and the interaction between bubbles. As shown next, the SMT predictions furnish very good results as compared with the slug tracking method, the new approach being much simpler and faster. A comparison between the two methods yields a gain on computing time of two orders of magnitude.

2. Closure relations

Any model that aims at predicting the flow structure needs to resort to a number of closure laws, in particular, to express bubble velocity and shape.

2.1. Bubble velocity in fully developed flow

The velocity of a long bubble in a fully developed horizontal slug flow was extensively studied in the past. This velocity can be expressed through the equation proposed by Nicklin et al. (1962) (vertical flow):

$$V = C_0 U + C_\infty \sqrt{gD}, \tag{1}$$

where V is the bubble nose velocity, U is the mixture velocity of the liquid slug ahead of the bubble, g is the gravity and D the pipe diameter. Nicklin et al. (1962) proposed $C_0 = 1.2$ for turbulent flow and $C_\infty = 0.35$.

For horizontal flow, Bendiksen (1984) proposed the use of two sets of coefficients, depending on the Froude number (F_r) defined as:

$$F_r = \frac{U}{\sqrt{gD}} \tag{2}$$

For Froude numbers above a critical value $F_{r_{crit}}$, C_0 is equal to 1.2 and the drift coefficient C_∞ vanishes. For low Froude numbers, C_0 is equal to unity and the drift coefficient becomes a function of the Eötvos number, as proposed by Moissis and Griffith (1981):

$$C_\infty = 0.54 - 1.76 E_o^{-0.56}, \tag{3}$$

where the dimensionless number E_o is defined as:

$$E_o = \frac{(\Delta\rho) g D^2}{\sigma} \tag{4}$$

and σ and ρ are, respectively the superficial tension and density.

To ensure continuity, the critical Froude number is

$$Fr_{critical} = \frac{0.54 - 1.76 E_o^{-056}}{0.2} \tag{5}$$

For air and water flowing in a 53 mm pipe section at atmospheric pressure, the Eötvos number is about 390. In this case, the coefficients of Eq. (1) are:

$$\begin{aligned} &C_0 = 1.0 \text{ and } C_\infty = 0.48 \quad \text{for } U < 2.4\sqrt{gD} \\ &C_0 = 1.2 \text{ and } C_\infty = 0 \qquad \text{for } U \geq 2.4\sqrt{gD} \end{aligned} \tag{6}$$

2.2. Influence of the slug length on the bubble velocity

Moissis and Griffith (1962) presented the first study on the influence of the liquid slug length on bubble velocity. These authors studied vertically ascendant flows to propose

$$v(L_S) = 8.0 e^{-1.06 L_S/D}, \tag{7}$$

where variable L_S is the length of the liquid slug that precedes the bubble whose dimensionless velocity v and is defined as

$$v(L_S) = \frac{V_B - V_{B_\infty}}{V_{B_\infty}} \tag{8}$$

The velocity V_B is the actual bubble nose velocity and V_{B_∞} is the bubble nose velocity behind an infinite long liquid slug ($L_S \to \infty$).

Several authors used their own results to calibrate equations with the basic format of Eq. (7), including horizontal flows.

Nydal and Banerjee (1996) proposed a slug-tracking model that is deemed valid for any pipe inclination and adopts Eq. (7) in its original format. Barnea and Taitel (1993) used a similar expression, but with different coefficients for the horizontal case; the proposed expression was

$$v(L_S) = 5.5 e^{-6.0 L_S/L_{STAB}}, \tag{9}$$

where L_{STAB} is the minimum length of a stable slug and was considered equal to $10D$ for the tested low mixture velocity ($0.26\,\mathrm{ms}^{-1}$) and $15D$ for the tested higher velocity ($1.5\,\mathrm{ms}^{-1}$).

Grenier (1997) also proposed a slug-tracking model for the horizontal case. The proposed expression for bubble velocity was based on Eq. (7), with modified coefficients as to better fit his experimental data on the flow of water and air in a pipe with 53 mm internal diameter and 90 m in length. The expression used by Grenier (1997) was

$$v(L_S) = 0.4 e^{-0.5 L_S/D} \tag{10}$$

Cook and Behnia (2000) presented an article comparing their slug-tracking model with experimental results obtained in a horizontal pipe with 50 mm i.d. and 16 m in length. The data were obtained at a position 10 m downstream of the inlet position. For their slug-tracking model, they proposed the following relation between bubble velocity and slug length

$$v(L_S) = 0.56 e^{-0.46 L_S/D} \tag{11}$$

Fagundes Netto et al. (2001) carried out an experimental study on the behavior of two isolated air bubbles traveling in water flow and separated by a short distance. The test section consisted of a 90 m horizontal pipe with 53 mm internal diameter. A system of control valves allowed the injection of bubbles with a given length and separating distance. Capacitance sensors were distributed at two measuring positions (3 and 65 m downstream of the inlet location) to evaluate the size of the bubbles, their velocities and separating length. The experiments show that bubbles separated by liquid slugs shorter than a critical value coalesce. Conversely, for liquid slugs bigger than the critical value, the trailing bubbles were observed to move slower than the leading bubbles so that the distance between them increased.

Fig. 1 shows the experimental data of Fagundes Netto et al. (2001) on L_S/D at positions 3 (x-axis) and 65 (y-axis) meters downstream of the flow inlet. The graph basically illustrates the distance between two consecutive bubbles at these two

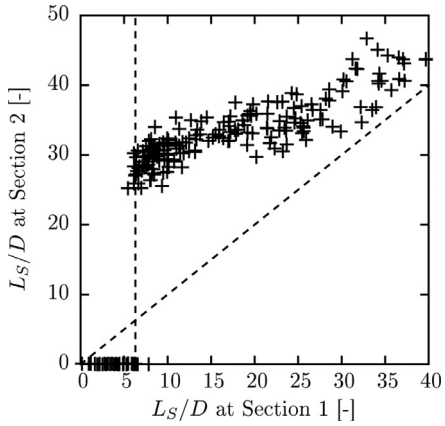

Fig. 1. Evolution of slug length at positions 3 m (Section 1) and 65 m (Section 2) from the inlet. Data of Fagundes Netto et al. (2001).

positions. Provided at position 3 m, the distance between the two bubbles is shorter than 6.3D, coalescence occurs so that $L_S/D = 0$ at 65 m. On the other hand, for $L_S/D > 6.3D$, the distance between bubbles increases, evidencing that the trailing bubble moves slower than the leading bubble. The data, in particular, suggests that an exponential relationship between bubble velocity and slug length, as proposed by Moissis and Griffith (1962) for vertical flow, is not appropriate for horizontal flow. To overcome this difficulty, Fagundes Netto et al. (2001) proposed the relation:

$$v(L_S) = 0.22[1 - L_S/(6.3D)]e^{-0.16(L_S/D)} \tag{12}$$

2.3. The coalescence process

Most of the slug tracking models do not consider the actual shape of the bubbles and consider that, in the event of coalescence, the resulting bubble length is the sum of the two original bubbles lengths.

However, Fagundes Netto (1999) has shown that as two bubbles merge in a horizontal flow, the length of the resulting bubble is smaller than the sum of their lengths. The reduction in length is caused by the drainage of the liquid film originally located under the nose of the trailing bubble. To estimate this difference (ΔL_C) the following correlation was advanced:

$$\frac{\Delta L_C}{D} = 1.225\left(1 - \frac{1}{\sqrt{Fr}}\right)\left(\frac{L_{B1} + L_{B2}}{2D}\right)^{2/3}, \tag{13}$$

where L_{B1} and L_{B2} are the lengths of the two original bubbles and D is the pipe diameter.

In the present work this equation is modified to:

$$\frac{\overline{\Delta L_C}}{D} = 1.225\left(1 - \frac{1}{\sqrt{Fr}}\right)\left(\frac{\overline{\Delta L_B}}{D}\right)^{2/3} \tag{14}$$

3. Slug flow models

3.1. Unit cell

Unit cell models estimate the averaged slug flow parameters by approximating the transient, chaotic phenomenon through a steady periodic structure that is repeated downstream. As mentioned before, distinct models are available in literature, based on hypotheses that may exhibit considerable differences. Gonçalves et al. (2018) discuss in detail the physical hypotheses and the mathematical constrains that support the models of Dukler and Hubbard (1975) and Orell (2005). As it turns out, the model of Orell (2005) is of easier numerical implementation and has a "bigger" validity domain (please refer to Gonçalves et al., 2018 for a discussion on the *physical* and *feasible* validity domains of unit cell models). The models analyzed in Gonçalves et al. (2018) had their full physical and mathematical formulations (with adequate notation) explained in Bandeira et al. (2017). For a detailed description on the formulation of the models of Dukler and Hubbard (1975) and Orell (2005) the reader is referred to the origin sources or to Bandeira et al. (2017).

The model of Orell (2005) combines a separated flow region in which the film region is described as a flat, stratified geometry and a mixture model in the slug region. The model furnishes prediction for the average holdup and pressure drop. Specifically, the model yields slug and bubble fractions L_S/L_u and L_B/L_u. For comparison with the other methods, a formulation for the frequency of passage of slugs is required so that the quantity $L_u = U_t/v_s$ can be estimated; here, the correlation of Schulkes (2011) is used. This correlation is relatively new and is based on an ample data set with 1200 experimental points. The expression takes into account the dynamic and geometric properties of flows and is given by

$$v_s = \Psi(\alpha)\Phi(Re_L)\Theta(\theta, Fr_L)\frac{U}{D}, \tag{15}$$

where α = flow volumetric gas fraction, Re_L = liquid slug Reynolds number, Fr_L = liquid slug Froud number, θ = pipe slope.

The auxiliary functions are defined through:

$$\Psi(\alpha) = 0.016\alpha(2 + 3\alpha) \tag{16}$$

$$\Phi(Re_L) = \begin{cases} 12.1Re_L^{-0.37}, & Re_L < 4000 \\ 1.0, & Re_L \geq 4000 \end{cases} \tag{17}$$

$$\Theta(\theta, Fr_L) = \begin{cases} 1 + \frac{2}{Fr_L}\text{sgn}(\theta)\sqrt{|\theta|}, & |\theta| \leq 0.17 \\ \frac{1.8}{Fr_L}(0.6 + 2\theta - \theta^2), & |\theta| > 0.17 \end{cases} \tag{18}$$

3.2. Slug tracking

The model of Cook and Behnia (2000) is based on the work of Barnea and Taitel (1993). Both models determine the statistical distribution of slug lengths from an empirical expression that defines the rate of collapse of short slugs as a function of their lengths; their basic distinction is the specification of distinct evolution laws. Cook and Behnia (2000) used their own experimental data whereas Barnea and Taitel (1993) fitted the data of Moissis and Griffith (1962). The model is purely evolutionary. Once the translational velocities of the front and rear of randomly distributed slugs are assigned through the working empirical expressions, the motion of the slug can be described through a simple marching process. The models at no instant resort to the first principles; thus, no dynamic equation of motion is solved.

The position of a slug rear (R) and front (F) is updated through the propagation equations:

$$R_i^{t+\Delta t} = R_i^t + V_{R_i}\Delta t \tag{19}$$

where V_R is the velocity of a bubble behind a slug (obtained from Eq. (11)) and

$$F_i^{t+\Delta t} = F_i^t + V_{F_i}\Delta t \quad \text{and} \quad V_{F_i} = V_{R_{i-1}} \tag{20}$$

respectively.

A slug collapses as R_i approaches F_i. As a natural consequence of this event, the collapsed slug is removed from the pipe and all upstream cells are renumbered (Cook and Behnia, 2000).

The length of each individual slug is given by:

$$(L_S)_i = F_i - R_i \tag{21}$$

3.3. Slug capturing

The slug capturing approach aims at naturally reproducing the physics of slug generation through the solution of a two-fluid model for separated flow. The method was introduced by Issa and Kempf (2003) and has been further applied successfully by other authors for the prediction of slug length distributions (see, e.g., Nieckele et al., 2013).

The model considered here in based on the formulation of Evje and Flåtten (2003). The continuity equation for each phase $k(= G, L)$ is given by:

$$\frac{\partial(\rho_k \alpha_k)}{\partial t} + \frac{\partial(\rho_k \alpha_k U_k)}{\partial x} = 0 \tag{22}$$

The momentum conservation equation assumes the form:

$$\frac{\partial(\rho_k \alpha_k U_k)}{\partial t} + \frac{\partial}{\partial x}(\rho_k \alpha_k U_k^2 + (p_k - p_k^i)) + \alpha_K \frac{\partial p_k^i}{\partial x} = Q_k, \tag{23}$$

where p_i^k is the pressure at the gas-liquid interface, and Q_k represents the momentum sources due to gravity and friction.

The friction factors follow the recommendations of Issa and Kempf (2003); the expressions of Taitel and Dukler (1976) are chosen for the calculation of gas-wall and interfacial stresses, and for the liquid-wall term, the correlation of Spedding and Hand (1997) is used.

Once the volume fraction and velocity field solutions have been obtained, a post-processing procedure has to be applied to determine whether each position is part of a liquid slug or a gas long bubble. A region was considered to be part of a liquid slug when the liquid holdup was over the threshold of 98%.

4. Experimental studies: Data for model validation

4.1. Grenier (1997)

Grenier (1997) studied experimentally the evolution of the slug flow structure in horizontal pipes. His experiences were performed with water and air in a 90 m PVC transparent pipe with 53 mm of internal diameter. The system was kept at atmospheric pressure and the four measurement stations were located at 24, 44, 64 and 84 m from the injection point. Two different injection systems were used: a horizontal "Y" connection where the gas phase flowed in the upper branch and a system where liquid and gas were mixed at the bottom of a vertical 2.5 m pipe, the end of which was connected to the horizontal test pipe.

Several tests were carried out, with changes in the injection system and the flow rates of the phases. To every condition, a large enough number of bubbles and slugs was considered to ensure a reliable estimation of statistical parameters.

Grenier (1997) noted that the type of injection has no influence on the flow structure downstream of 24 m from the injection point. He suggested that the structure formation of slug flows is such that the initial condition is somehow forgotten after a certain development length. The evolution of the bubble and slug length distributions along the pipe was also analyzed by Grenier. He observed that the coalescence process is very active in the slug formation region, resulting in an increase in bubble and slug mean lengths. Downstream of the 44 m mark, the coalescence process disappears and the mean slug length becomes constant. The slug length standard deviation, however, always decreased along the last half part of the pipe. Grenier referred to this phenomenon as a "calibration process", which was observed in every studied case.

4.2. Cook and Behnia (2000)

Cook and Behnia (2000) performed experiments for the assessment of slug length distributions in a near-horizontal pipe. The apparatus consisted of a 16 m long transparent tube, with 50 mm internal diameter. Experiments were performed with air and water; the authors measured the slug length distributions at a section positioned 11 m downstream of the inlet. Measurements were performed through conductance probes, for three operational conditions.

4.3. Ujang et al. (2005)

Ujang et al. (2006) evaluated the effects of pressure (1, 4 and 9 bar) and superficial velocities on the distributions of slug lengths and the time intervals between slug arrivals. The flows were of air in water. The test section was a 37 m horizontal pipe, with internal diameter of 78 mm. Measurements were performed using conductive probes, at 14 positions.

In the present work, the three experiments performed at near atmospheric pressure are considered for comparison with model predictions. The authors do not furnish the averaged statistics for the measured quantities, showing instead the parameters of the fitted distributions. Following Gonçalves et al. (2018), the means and standard deviations of the data were estimated from the properties of the log-normal distribution.

4.4. Mayor et al. (2008)

The studies of Mayor et al. (2008) were conducted in a vertical pipe for air-water co-current slug flow. The experiments were performed in 6.5 m acrylic columns with internal diameters of 32 and 52 mm (Table 2). The experimental data were collected at two positions, 3.25 and 5.40 m from the base of the column. The superficial gas and liquid velocities were varied up to the maximum values of 0.26 and 0.20 ms^{-1} respectively.

The expansion of the gas in the column was estimated disregarding the pressure drop due to the effects of friction at the wall and the wake of the bubbles. Therefore, the pressure distribution along the column considers only the hydrostatic pressure gradient.

4.5. Gonçalves et al. (2018)

To compare different methodologies for estimation of slug properties distributions, Gonçalves et al. (2018) performed experiments of air and water in an horizontal tube with 12 m length and internal diameter of 44.2 mm. Liquid and gas superficial velocities ranged from 0.72 ms^{-1} to 1.81 ms^{-1} and 0.2 ms^{-1} to 0.8 ms^{-1}, respectively. Bubble and slug lengths were measured through a Shadow Sizer System.

4.6. Van Hout et al. (2003)

van Hout et al. (2003) measured bubble velocity and slug and bubble length distributions in inclined pipes with internal diameters of 24 and 54 mm and total length of 10 m. Inclination varied between 2–90° from the horizontal, and measurements were performed in several positions along the pipe.

The authors present comparisons with theoretical predictions for inclinations of 10, 30 and 90°, for the operational conditions of $U_{SL} = 0.01\ ms^{-1}$, $U_{SG} = 0.41\ ms^{-1}$, $D = 24$ mm; the same set of conditions was considered for the validation herein.

4.7. Summary of experimental conditions

A summary of the horizontal and vertical experimental conditions discussed in the present work is presented in the flow pattern maps introduced in Fig. 2.

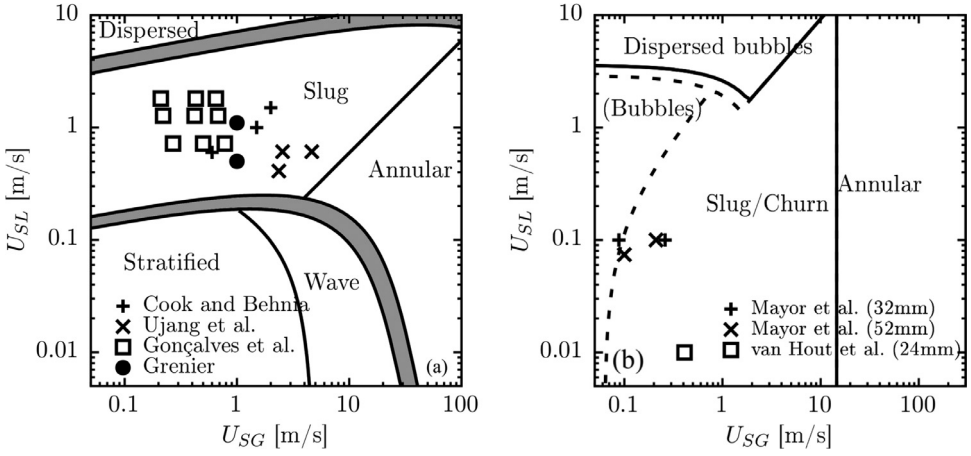

Fig. 2. Summary of the experimental flow conditions. (a) Horizontal flow pattern (Taitel and Dukler, 1976). (b) Vertical flow pattern (Taitel et al., 1980).

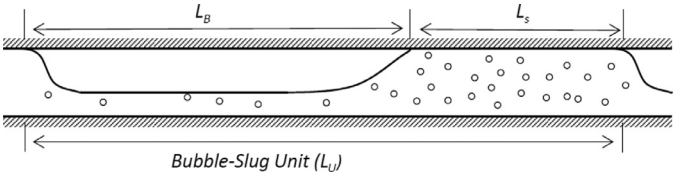

Fig. 3. Unit cell.

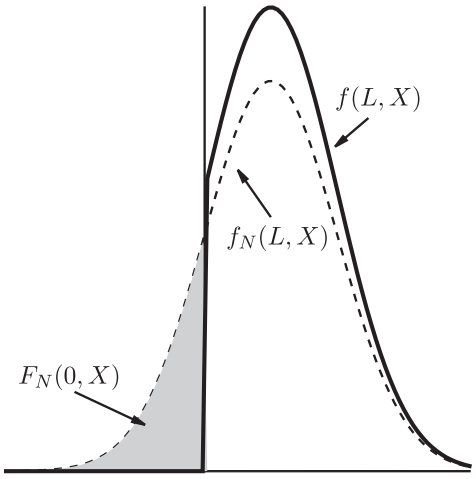

Fig. 4. PDF functions.

5. The statistical moments transport model

Slug-tracking models transport individual long bubbles downstream a pipe. The simulation time must then be such as to ensure the passage, at each pipe position, of a number of bubbles large enough to allow a reliable estimation of statistical parameters. The entire process is normally very time-consuming. To avoid this problem, a completely new approach is proposed, based on equations that are set to transport directly the statistical moments, rather than individual bubbles.

5.1. Definitions

A unit cell is defined as a bubble and the upstream liquid slug, as shown in Fig. 3. The variable x represents the cell location, referred from the pipe inlet.

Let $L_S(x, i)$ be the length of the ith liquid slug observed at position x. For a fixed observer, the flow is composed of a time sequence of unit cells. L_S is then the random variable that represents the liquid slug length and its statistical distribution can be estimated at any pipe position.

The distribution function $F(L_S, x_0)$ represents the probability of having a liquid slug shorter than L_S at position x_0 of the pipe:

$$F(L_S, x_0) = P_B(L \leq L_S; x = x_0) \tag{24}$$

The probability density function (PDF), $f(L_S, x_0)$, is defined as:

$$f(L_S, x_0) = \left.\frac{\partial F}{\partial L_S}\right|_{x_0} \tag{25}$$

These two functions are defined only for positive values of L_S. To represent properly this condition, the PDF may be written as:

$$f(L_S, x) = \frac{H(L_S) f_N(L_S, x)}{1 - F_N(0, x)}, \tag{26}$$

where $H(L_S)$ is the Heaviside function and f_N is a continuous PDF function defined in $(-\infty, +\infty)$.

Coalescence occurs as $L_S \rightarrow 0$. To capture the coalescence of bubbles, $f(0, x)$ must be greater than zero. The implication is that the model fails if Lognormal or Inverse-Gaussian distributions are used.

Function $f(L_S, x)$ is thus normalized and reduced to zero for negative values of L_S (Fig. 4).

Another modeling possibility would be to consider a minimum stable L_S instead of 0. By this manner, a slug length below which slugs disintegrate could be defined, say, one or two pipe diameters. Through this artifice, log-normal distributions could then be used (log-normal distributions are notoriously the most likely distributions for slug length).

5.2. Coalescence rate

The usefulness of the present approach depends sensitively on a proper description of the coalescence process and its influence on the flow structure evolution. The first step is to define a coalescence rate, Γ_C, that measures the relative number of liquid slugs that disappear per unit of pipe length:

$$\Gamma_C = -\frac{1}{N}\frac{\delta N}{\delta x} \tag{27}$$

The coalescence rate is equal to the probability P_B of disappearance of a slug in an observation window of length dx, divided by

this length, or, in limit terms,

$$\Gamma_C(x_0) = \lim_{\Delta x \to 0} \frac{P_B(L \le 0; x = x_0 + \Delta x)}{\Delta x} \tag{28}$$

However,

$$\begin{aligned} P_B(L \le 0; x = x_0 + \Delta x) &= P_B(L \le -(dL/dx)\Delta x; x = x_0) \\ &= F(-(dL/dx)\Delta x; x = x_0)) \\ &\cong -f(0; x_0)(dL/dx)|_{(0;x_0)}\Delta x \end{aligned} \tag{29}$$

Based on the above definition, the coalescence rate represents the probability of collapse of slug units within an observation window of width δx, so that,

$$\Gamma_C(x_0) = -f(0, x_0)\left.\frac{dL_s}{dx}\right|_{(0;x_0)}, \tag{30}$$

$$\Gamma_C(x_0) = f(0, x_0)\frac{\nu(0) - \overline{\nu(L_S)}}{\overline{\nu(L_S)} + 1} \tag{31}$$

and the overline indicates an averaged value.

5.3. General equation for the SMT model

The transport equations for liquid slugs and large bubbles are derived next. They are used as basis for the introduction of a general transport equation.

5.3.1. Transport equation for the length of liquid slugs

Let $Y(L, x)$ be any function of the slug length L at any position x of the pipe; its average is a function of the pipe position x and is given by

$$\overline{Y(x)} = \int_{-\infty}^{\infty} Y(L) f(L; x) dL \tag{32}$$

The gradient of $Y(x)$ may then be written as

$$\frac{d\overline{Y(x)}}{dx} = -\frac{\int_{-\infty}^{\infty} Y(L) H(L) \frac{\partial L}{\partial x} \frac{\partial f_N}{\partial L} dL}{1 - F_N(0, x)} + \Gamma_C \overline{Y} \tag{33}$$

with

$$\Gamma_C = \frac{1}{1 - F_N(0, x)} \left(\frac{\partial F_N}{\partial L_s} \frac{\partial L_s}{\partial x} \right)\Bigg|_{(0,x)} \tag{34}$$

Solving the integral by parts and realizing that f_N vanishes for $L_s = \pm\infty$, one gets

$$\frac{d\overline{Y(x)}}{dx} = \overline{Y' \frac{\partial L_s}{dx}} + \frac{1}{1 - F_N(0, x)} \left(\frac{\partial L_S}{\partial x} f_N \right)\Bigg|_{(0,x)} \overline{Y_0} + \Gamma_C \overline{Y}, \tag{35}$$

where $\overline{Y_0}$ is the average of Y considering just those cell units whose slug lengths tend to zero.

Eq. (33) is then cast as

$$\frac{d\overline{Y(x)}}{dx} = \Gamma_C(\overline{Y} - \overline{Y_0}) + \overline{\left(\frac{dY}{dx}\right)} \tag{36}$$

5.3.2. Transport equation for the length of long bubbles

To describe the behavior of long bubbles consider Y a function of L_B. After the observation of a sufficiently large number of bubbles, one may write

$$\overline{Y} = \frac{1}{N} \sum_{i=1}^{N} Y_i \tag{37}$$

The derivative of the above expression is readily shown to be

$$\frac{d\overline{Y}}{dx} = -\frac{1}{N}\frac{dN}{dx}\left(\frac{1}{N} \sum_{i=1}^{N} Y_i - \frac{d\sum_{i=1}^{N} Y_i}{dN} \right) + \frac{1}{N} \sum_{i=1}^{N} \frac{dY_i}{dx} \tag{38}$$

that is

$$\frac{d\overline{Y(x)}}{dx} = \Gamma_C(\overline{Y} - \overline{Y_0}) + \overline{\left(\frac{dY}{dx}\right)} \tag{39}$$

with

$$\overline{Y_0} = \frac{d\sum_{i=1}^{N} Y_i}{dN} \tag{40}$$

5.4. General equation

Quantity Y changes with position due to at least three effects: pressure drop, bubble-bubble interaction and coalescence, that is,

$$\overline{\left(\frac{dY}{dx}\right)} = \overline{\left(\frac{dY}{dx}\right)}_P + \overline{\left(\frac{dY}{dx}\right)}_I + \overline{\left(\frac{dY}{dx}\right)}_C \tag{41}$$

As coalescence occurs, an entire unit cell disappears and the following unit increases in size. If L_s^* represents the slug length of the precedent unit, one may write:

$$\overline{\left(\frac{dY}{dx}\right)}_C = \delta(L_S^*)\frac{dL_S^*}{dx}(Y_{after} - Y_{before}), \tag{42}$$

where Y_{after} and Y_{before} are the values of Y of the unit that follows the one that disappears, immediately after and before the coalescence process, respectively.

The general equation for the Statistical Moments Transport Model is given by:

$$\frac{d\overline{Y}}{dx} = \Gamma_C(\overline{Y} + \overline{\Delta_C Y}) + \overline{\left(\frac{dY}{dx}\right)}_P + \overline{\left(\frac{dY}{dx}\right)}_I, \tag{43}$$

where Δ_C Y is the difference between the value of Y of a slug unit resulting from coalescence and the sum of the Y values of the two original cells.

$$\Delta_C Y = Y_{\text{after}} - (Y_0 + Y_{\text{before}}) \tag{44}$$

The coalescence of bubbles impacts the statistical moments through two effects: (i) it reduces the number of slug units and, consequently, increases the average length, (ii) the length of the resulting bubble after coalescence is smaller than the sum of the two original bubble lengths. As a corollary, the resulting liquid slug is bigger than the original slug due to the drainage of the liquid under the nose of the trailing bubble.

The last two RHS terms of Eq. (43) represent the influence on Y of the pressure and of the interaction between bubbles.

5.5. Hypotheses

The following hypotheses are considered in this work:

1. The pressure gradient dP/dx in the pipe is known. As a result of this hypothesis, the present formulation must be complemented by one of the several available methods in literature to estimate the pressure evolution. For example, unit cell models such as those described in either Dukler and Hubbard (1975) or Orell (2005) can be used.
2. The liquid slug length is not affected by depressurization. This hypothesis results from two other hypotheses: (i) the liquid slug is free from aeration, (ii) the liquid is incompressible.
3. Liquid slugs that immediately follow those that disappear have the same average length than the totality of slugs.
4. Bubble and slug lengths are two independent random variables. The lengths of liquid slugs and bubbles are correlated in the entrance region of a pipe. As the flow develops downstream and successive bubble coalescence occurs, any

existing variable dependence tends to be weakened. To simplify the present model, the lengths of liquid slugs and bubbles were considered independent random variables
5. As coalescence occurs, the lengths of leading and trailing bubbles are two independent random variables.
6. Bubbles that immediately follow slugs that disappear have the same average length than the total added lengths of bubbles.
7. Bubbles that immediately precede slugs that disappear have an average length shorter than the total added lengths of bubbles.

5.6. Average and standard deviation of bubble and slug lengths

Eq. (43) must be developed for $Y = L_S$, L_B, $(L_S - \overline{L_S})^2$ and $(L_B - \overline{L_B})^2$.

As a result, expressions may be developed for the evolution of the mean and standard deviation of slug and bubble lengths.

5.7. Mean slug length

Under the previous hypotheses and for $Y = L_S$, Eq. (43) becomes:

$$\frac{d\overline{L_S}}{dx} = \Gamma_C(\overline{L_S} + \overline{\Delta_C L_S}) + \overline{\left(\frac{dL_S}{dx}\right)_I} \tag{45}$$

The last term is due to the interaction between bubbles, i.e., to the difference between the velocities of leading and trailing bubbles.

For one particular slug, one may write:

$$\left(\frac{dL_S}{dx}\right)_I = v(L_S^*) - v(L_S), \tag{46}$$

where v represents the interaction law given by any equations from Eqs. (7)–(11) and $L_S^*$is the length of the slug of the previous cell. As L_S and L_S^* have obviously the same distribution, the mean value of this term is equal to zero. Therefore,

$$\frac{1}{\overline{L_S}}\frac{d\overline{L_S}}{dx} = \Gamma_C\left(1 + \frac{\overline{\Delta_C L_S}}{\overline{L_S}}\right) \tag{47}$$

This expression shows that the average slug length only changes when coalescence occurs.

5.8. Slug length standard deviation

The evolution of the slug length variance is obtained doing $Y = (L_S - \overline{L_S})^2$. Just before coalescence, the two slug lengths are 0 and L_{S0}. Hypothesis 3 leads to:

$$\begin{aligned}\overline{\Delta_C Y} &= \overline{\left[(L_{S0} + 0 + \overline{\Delta_C L}) - \overline{L_S}\right]^2 - \left[(L_{S0} - \overline{L_S})^2 + (0 - \overline{L_S})^2)\right]} \\ &= \overline{\Delta_C L}^2 - \overline{L_S}^2\end{aligned} \tag{48}$$

and

$$\begin{aligned}\left(\frac{dY}{dx}\right)_I &= 2(L_S - \overline{L_S})\left[\left(\frac{dL_S}{dx}\right)_I - \left(\frac{d\overline{L_S}}{dx}\right)_I\right] \\ &= 2(L_S - \overline{L_S})\left(\frac{dL_S}{dx}\right)_I\end{aligned} \tag{49}$$

Using Eq. (46), the average is then

$$\begin{aligned}\overline{\left(\frac{dY}{dx}\right)_I} &= \overline{2(L_S - \overline{L_S})\left(\frac{dL_S}{dx}\right)_I} \\ &= 2\overline{L_S(v(L_S^*) - v(L_S))} - \overline{L_S}\overline{\left(\frac{dL_S}{dx}\right)_I}\end{aligned} \tag{50}$$

The last term of Eq. (50) is zero, as seen before.

$$\overline{\left(\frac{dY}{dx}\right)_I} = 2(\overline{L_S v(L_S^*)} - \overline{L_S v(L_S)}) \tag{51}$$

Since L_S and L_S^* are independent variables,

$$\overline{\left(\frac{dY}{dx}\right)_I} = 2(\overline{L_S}\,\overline{v(L_S^*)} - \overline{L_S v(L_S)}) \tag{52}$$

and Eq. (53) follows immediately,

$$\begin{aligned}\frac{1}{\sigma_S^2}\frac{d\sigma_S^2}{dx} &= \frac{1}{\sigma_S^2}\frac{d\overline{(L_S - \overline{L_S})^2}}{dx} \\ &= \Gamma_C\left(1 + \frac{\overline{\Delta_C L}^2 - \overline{L_S}^2}{\sigma_S^2}\right) + 2\frac{\overline{L_S}\,\overline{v(L_S)} - \overline{L_S v(L_S)}}{\sigma_S^2}\end{aligned} \tag{53}$$

or

$$\frac{1}{\sigma_S}\frac{d\sigma_S}{dx} = \frac{\Gamma_C}{2}\left(1 + \frac{\overline{\Delta_C L}^2 - \overline{L_S}^2}{\sigma_S^2}\right) + \frac{\overline{L_S}\,\overline{v(L_S)} - \overline{L_S v(L_S)}}{\sigma_S^2} \tag{54}$$

5.9. Bubble length average

For $Y = L_B$, the general equation becomes

$$\frac{dL_B}{dx} = \Gamma_C(\overline{L_B} + \overline{\Delta_C L_B}) + \overline{\left(\frac{dL_B}{dx}\right)_P} \tag{55}$$

As coalescence occurs, the resulting bubble is shorter than the sum of the two original bubble lengths,

$$\overline{\Delta_C L_B} = -\overline{\Delta_C L_S} \tag{56}$$

The bubble length gradient due to depressurization depends on the pressure and the pressure gradient at position x, its length L_B and the ratio between the mean void fraction in the film region $\overline{\alpha_G}$ and the void fraction at the bubble tail, α_{GT}. Considering ideal gas:

$$\left(\frac{d\overline{L_B}}{dx}\right)_P = \frac{1}{A\alpha_{GT}}\frac{dW_B}{dx} = -\frac{W_B}{A\alpha_{GT}}\frac{1}{P}\frac{dP}{dx} = -\frac{A\overline{\alpha_G}L_B}{A\alpha_{GT}}\frac{1}{P}\frac{dP}{dx} \tag{57}$$

or

$$\left(\frac{dL_B}{dx}\right)_P = C_S\frac{L_B}{L_P}, \tag{58}$$

where $L_P = -P/((dP)/dx)$ is a characteristic length, constant for a given position x. W_B is the bubble volume and A the pipe section. The coefficient C_S is defined as:

$$C_S = \frac{\overline{\alpha_G}}{\alpha_{GT}} \tag{59}$$

This coefficient depends on the bubble length, the liquid velocity in the slug and the bubble velocity. Fagundes Netto (1999) proposes to consider C_s constant and equal to 0.85.

Differently from the slug length, the mean bubble length changes not only because of coalescence but also due to pipe depressurization:

$$\frac{1}{\overline{L_B}}\frac{d\overline{L_B}}{dx} = \Gamma_C\left(1 - \frac{\overline{\Delta_C L_S}}{\overline{L_B}}\right) + C_S\frac{1}{L_P} \tag{60}$$

5.10. Bubble length standard deviation

To obtain the evolution of the bubble length variance, $Y = (L_B - \overline{L_B})^2$,

$$\overline{\Delta_C Y} = \overline{\left[(L_{B1} + L_{B2} - \overline{\Delta_C L}) - \overline{L_B}\right]^2 - \left[(L_{B1} - \overline{L_B})^2 + (L_{B2} - \overline{L_B})^2\right]} \tag{61}$$

Under Hypotheses 5, 6 and 7, Eq. (61) may be simplified to

$$\overline{\Delta_C Y} = (\overline{L_B} - \overline{\Delta_C L})(C_B \overline{L_B} - \overline{\Delta_C L}), \tag{62}$$

where $C_B = (2\ \lambda\ -\ 1)$ and λ is the ratio between the average length of the bubbles that precede a slug that coalesces and the average overall bubble length ($\overline{L_{B2}} = \lambda \overline{L_B}$).

Grenier (1997) measured the structure of the flow at different positions in the pipe. He reported that close to the injection point, where coalescence is observed, the bubble length is strongly correlated with the following slug length. In other words, short slugs follow short bubbles and long slugs follow long bubbles. He also observed that the slugs that disappear are the shortest. The conclusion is that bubbles reached by trailing bubbles are, in average, shorter than the total length of bubbles. Based on his experimental observations and on results obtained through a slug-tracking model, Grenier (1997) established the mean length of these bubbles to be about 60 to 75% of the global average length. In the present model, the best results were achieved using $\lambda = 2/3$ so that $C_B = 1/3$.

The pressure dependent term may be written as

$$\overline{\left(\frac{dY}{dx}\right)_P} = \overline{2(L_B - \overline{L_B})\left(\frac{dL_B}{dx}\right)_P} = 2\frac{C_S}{L_P}\overline{L_B(L_B - \overline{L_B})} = 2\frac{C_S}{L_P}\sigma_B^2 \tag{63}$$

The general equation becomes

$$\frac{1}{\sigma_B}\frac{d\sigma_B}{dx} = \frac{\Gamma_C}{2}\left(1 + \frac{(\overline{L_B} - \overline{\Delta_C L})(C_B \overline{L_B} - \overline{\Delta_C L})}{\sigma_B^2}\right) + \frac{C_S}{L_P}, \tag{64}$$

where $C_B = 1/3$ and $C_S = 0.85$.

5.11. Summary of the model

Given an initial distribution for both the bubble and slug lengths, the flow structure evolution may be estimated using the following equations:

1. The coalescence rate: Eq. (31).
2. The average slug length: Eq (47).
3. The slug length standard deviation: Eq. (54).
4. The average bubble length: Eq. (60).
5. The bubble length standard deviation: Eq. (64).

The following laws are proposed for use of the model:

1. Bubble-bubble interaction:
   (a) For vertical flow: Eq. (7)
   (b) For horizontal flow: Eq. (12)
2. Bubble shrinking due to coalescence
   (a) For vertical flow (cylindrical bubbles): $\overline{\Delta L_C}/D = 0$.
   (b) For horizontal flow: Eq. (14)

The modeling of the coalescence rate requires the specification of the probability density function f at $L_S = 0$. That is to say, a certain distribution law needs to be specified to determine the value of $f(0, x)$, given the mean value of L_S and the standard deviation σ_S. In literature, the normal consideration is that the liquid slug length is adequately described by Lognormal (Nydal et al. (1992) or Inverse-Gaussian (Dhulesia et al. (1991)) distributions. Unfortunately, both distributions vanish for L_S equal to zero so that they are unable to correctly represent the coalescence process. To avoid this problem, a Normal distribution defined only for positive values of L_S was used.

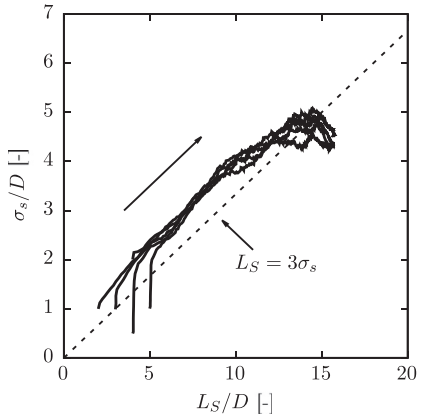

Fig. 5. Phase diagram on a plane defined by the mean value and the standard deviation of the liquid slug length according to the ST model of Grenier (1997). $j_L = 1.1\ \mathrm{ms}^{-1}$, $j_G = 1.0\ \mathrm{ms}^{-1}$.

The average value of $v(L_S)$ and $L_S v(L_S)$ are easily determined at any position x of the pipe:

$$\overline{v(L_S)} = \int_0^\infty v(L) f(L, x) dL \tag{65}$$

and

$$\overline{L_S v(L_S)} = \int_0^\infty L v(L) f(L, x) dL \tag{66}$$

6. Results

6.1. Influence of the initial condition

The data of Grenier (1997) suggests that the flow structure far away from the pipe inlet is independent of the initial length distribution observed immediately after the mixing point. A set of simulations were performed for fixed liquid and gas flow rates, and varying initial slug length distributions. Fig. 5 shows the results based on the *slug tracking (ST)* model. This figure represents the projection of the space of phases of the liquid slug length on a plane defined by the mean value and the standard deviation. The curves show that the trajectories of the structure evolution tend to the same asymptotic solution, where the mean value is constant while the standard deviation decreases. This behavior was repeatedly observed by Grenier (1997).

In Fig. 6 the same result is apparent as the SMT model is considered. The values estimated 30 m downstream of the inlet are shown; the conclusion, based on the model, is that the flow structure does not depend on the initial condition at a distance of about $x/D = 566$ downstream of the mixing point.

The behavior of the liquid slug distribution far from the inlet may be understood based on Eqs. (31), (47) and (54). The slug length becomes stable only as the coalescence rate vanishes. This occurs whenever the ratio between the mean slug length and its standard deviation is such that the probability density function at $L_S = 0$ is negligible. In fact, as $\overline{L_S} - 3\sigma(L_s) > 0$, one may consider $f(0) \approx 0$ for the majority of the usual distribution functions. In this case, the evolution of the standard deviation is described by the expression:

$$\frac{1}{\sigma_S}\frac{d\sigma_S}{dx} = \frac{\overline{L_S}\,\overline{v(L_S)} - \overline{L_S v(L_S)}}{\sigma_S^2} \tag{67}$$

To evaluate this term, consider that the slug length distribution is weakly dispersed around its average, so that the value of $v(L_S)$

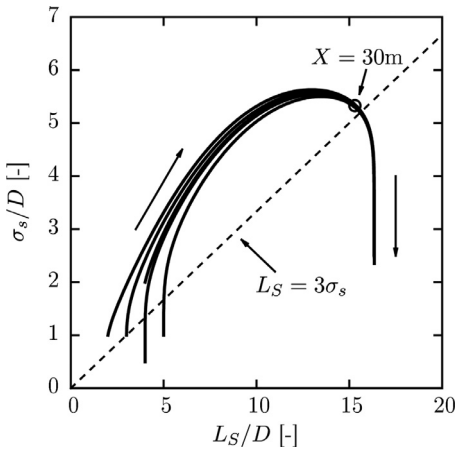

Fig. 6. Phase diagram on a plane defined by the mean value and the standard deviation of the liquid slug length according to the SMT model. $j_L = 1.1\,\mathrm{ms}^{-1}$, $j_G = 1.0\,\mathrm{ms}^{-1}$.

may be represented by the first two terms of a Taylor expansion centered on the mean slug length:

$$v(L_S) \approx v(\overline{L_S}) + (L - \overline{L_S})v'(\overline{L_S}) \tag{68}$$

A combination the above expressions leads to:

$$\frac{1}{\sigma_S}\frac{d\sigma_S}{dx} = -v'(\overline{L_S}) \tag{69}$$

Provided the function representing the interaction between bubbles is purely exponential, as suggested by Moissis and Griffith (1962), its derivative is always negative. In this case, the standard deviation always increases, the coalescence process is kept active and the average slug length increases. However, if an expression such as Eq. (12) is used instead, the derivative is always positive for L_S large enough. In this case, the standard deviation decreases with the pipe position, characterizing a phenomenon that aborts any possibility of further coalescence.

6.2. Model validation

The above remarks imply that unless experimental measurements are obtained at positions further downstream of about $x/D = 560$, the distributions of liquid slug and bubbles depend on the initial conditions. Unfortunately, most of the data available in literature do not fulfill this condition. This is the case for the data of Cook and Behnia (2000), Ujang et al. (2006), Mayor et al. (2008) and Gonçalves et al. (2018).

Hence, the comparison between the ST and SMT models is made in two parts. In the first part, results provided by both models are compared directly so that relative performances can be evaluated. In the second part, the SMT model is fully validated and compared to the other mentioned methods and experimental databases.

6.3. Numerical implementation details

Provided the flow statistics at several positions are available, the slug length distribution parameters - mean and standard deviation for the SMT, or minimum and maximum values for the ST - were adjusted as to reproduce as closely as possible the mean values of slug and bubble length at the most upstream station. Otherwise, the initial slug length is specified through an uniform distribution between 0 and 10D.

For horizontal flows, the initial bubble length was calculated with the expression proposed by Cook and Behnia (2000):

$$L_B = \frac{U_{SG}}{(1-\alpha_L)V - U_{SG}}L_S \tag{70}$$

where the mean film holdup α_L is given by:

$$\alpha_L = 1.4\frac{V-U}{V} \tag{71}$$

For vertical flows, the following expression was used:

$$L_B = \frac{U_{SG}}{U_{SL}}L_S \tag{72}$$

The ordinary differential equations were solved through the Runge-Kutta-Fehlberg method, which provides adaptive stepsize and error control. Absolute and relative tolerances of 10^{-2} and 10^{-4} were used, respectively. The step size was also limited so that positivity of the variables could be enforced.

The slug tracking calculation was implemented with a linked list to represent the unit cells. Bubbles were inserted in the domain until the statistics were converged and the number of samples k reached a minimum value of 30. The sampling was started as soon as the first cell left the pipe. The following criteria were used for the uncertainties ϵ_S and ϵ_B in the average slug and bubble lengths:

$$\epsilon_S = \frac{\sigma_S}{\sqrt{k}} < 10^{-2}\overline{L_S} \tag{73}$$

and

$$\epsilon_B = \frac{\sigma_B}{\sqrt{k}} < 10^{-2}\overline{L_B} \tag{74}$$

A step of 0.001 s was used for time advance.

6.4. Comparison of the SMT model with conventional slug tracking

The considerations introduced here for the implementation of the slug tracking methodology are very close to the closure equations and boundary conditions that are used in industrial codes. Hence, it is naturally expected that the present slug tracking computations provide results close to those otherwise obtained through industrial predictive codes.

To reproduce the results of the model proposed by Cook and Behnia (2000), a few adjustments are made.

1. The coalescence velocity is given by Eq. (11).
2. The inlet conditions are adjusted to match the slug tracking simulations.
3. The bubbles are considered cylindrical.
4. The pressure gradient is set to zero, meaning that compression effects are neglected.

A comparison between results obtained through the SMT and ST (C&B) methods is presented in Figs. 7 and 8. The maximum differences between mean slug and bubble lengths are less than 10% and 15%, respectively. The discrepancies may be attributed to the assumption of the normality of the slug length distribution and the simplifications regarding the conditional probabilities.

The distributions of liquid slug lengths are shown in Fig. 9. Again, the solutions agree very well, except for a small difference at L_s/D=10. The slug tracking model uses this value as a threshold for stable slugs, leading to a discontinuity in the coalescence velocity.

Since the SMT model directly provides the statistical features of the unit cells, likely it should exhibit a lower computational cost as compared to the stochastic simulations. To verify the scaling of the computational cost with domain size, the same conditions were used and the total pipe length was extended

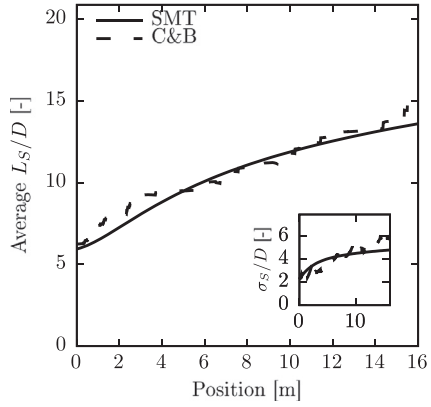

Fig. 7. Comparison of slug length results obtained through the SMT and ST (C&B) methods, with $U_{SL} = 0.6\,\mathrm{ms}^{-1}$, $U_{SG} = 0.6\,\mathrm{ms}^{-1}$. The inset figure shows the behavior of the standard deviation against position.

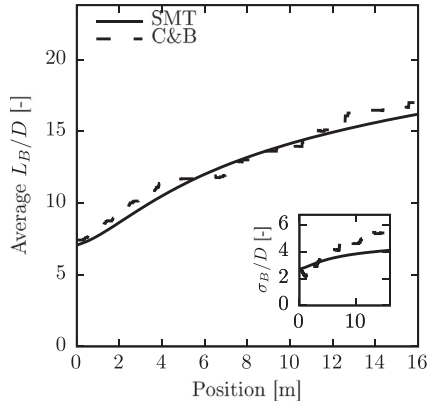

Fig. 8. Comparison of bubble length results obtained through the SMT and ST (C&B) methods, with $U_{SL} = 0.6\,\mathrm{ms}^{-1}$, $U_{SG} = 0.6\,\mathrm{ms}^{-1}$. The inset figure shows the behavior of the standard deviation against position.

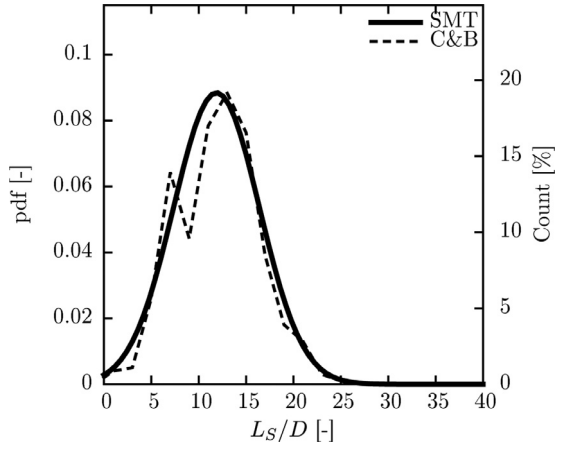

Fig. 9. Comparison of distributions of L_s/D obtained through the SMT and ST (C&B) methods, at $x = 10$m, with $U_{SL} = 0.6\,\mathrm{ms}^{-1}$, $U_{SG} = 0.6\,\mathrm{ms}^{-1}$.

from the original 16 m to modified values of 32 and 64 m. Fig. 10 shows a comparison of simulation running time, between the SMT and ST (C&B) methods. Time was normalized with the running time of the slug tracking simulation for a pipe length of 16 m. A reduction over ten fold in running time was observed between the SMT and ST (C&B) approaches. The computational cost for the SMT method barely increases with pipe length, while for the slug tracking method the increase in time is roughly proportional to

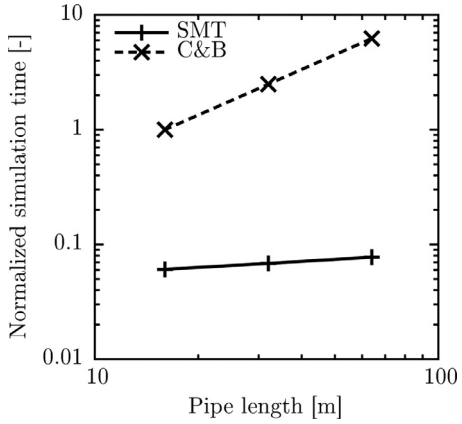

Fig. 10. Scaling of computational cost with pipe length for the SMT and ST (C&B) methods.

Table 1
The experimental data of Grenier (1997) for two distinct experimental conditions. The overline indicates an averaged value. σ stands for the mean-root squared value of an averaged quantity.

j_G	$(\mathrm{ms}^{-1})_{ATM}$	1.0	1.0
j_L	ms^{-1}	0.5	1.1
	$\overline{L_B}/D$	62.5	15.2
Station 1	σ_B/D	22.2	5.5
	$\overline{L_S}/D$	19.0	14.5
24 m	σ_S/D	6.9	4.8
	P (mbar)	1120	1350
	$\overline{L_B}/D$	68.9	18.4
Station 2	σ_B/D	23.8	6.6
	$\overline{L_S}/D$	20.5	17.0
44 m	σ_S/D	6.0	4.8
	P (mbar)	1096	1280
	$\overline{L_B}/D$	71.4	21.5
Station 3	σ_B/D	24.8	7.0
	$\overline{L_S}/D$	20.6	16.9
64 m	σ_S/D	5.46	4.3
	P (mbar)	1054	1180
	$\overline{L_B}/D$	73.8	23.8
Station 4	σ_B/D	20.3	7.6
	$\overline{L_S}/D$	25.1	17.0
84 m	σ_S/D	4.7	3.9
	P (mbar)	1020	1090

the domain size. For the 64 m simulations, a difference of two orders of magnitude in computing time was noted.

6.5. Validation of the SMT method against other procedures and experimental data

The present validation study was performed against a total of 21 data sets, from 5 different references.

In works where the experimental flow statistics were available, the inlet conditions for the numerical simulations of slug length predictions were adjusted to reproduce the mean and standard deviation as closely as possible. Otherwise, a uniform distribution with L_S ranging from 2 to 10D was considered.

The evolution of bubble and slug lengths predicted by the SMT and ST models were compared with the experimental results reported by Grenier (1997) and described in Table 1. In the following, the experimental data are represented by symbols. The dotted line represents predictions obtained through the ST model; results obtained with the SMT model are illustrated by the solid line.

Figs. 11–14 show that both SMT and ST models predict with good accuracy the measured $\overline{L_S}$, which is in turn not well predicted by the unit cell model. For the lower value of

Table 2
The experimental conditions of Mayor et al. (2008). H_L is the no slip hold up and dP/dx is the hydrodynamic pressure gradient considering no slip condition.

Cond.	ID (mm)	U_{LS} (ms^{-1})	U_{GS} (ms^{-1})	H_L	dP/dx
1	32	0.10	0.09	0.53	52.2
2	32	0.10	0.26	0.28	27.3
3	52	0.07	0.10	0.43	41.7
4	52	0.10	0.21	0.32	31.7

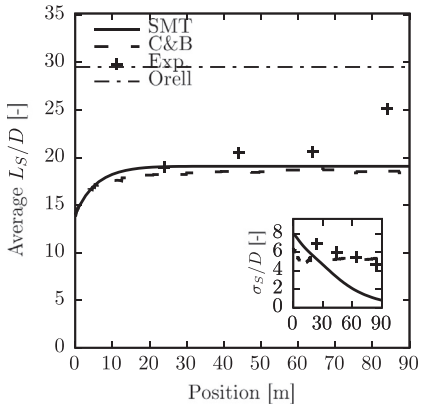

Fig. 11. Predictions of L_S/D for the experiment of Grenier (1997), with U_{SL} = 0.5 ms^{-1}, U_{SG} = 1.0 ms^{-1}. The inset figure shows the behavior of the standard deviation against position.

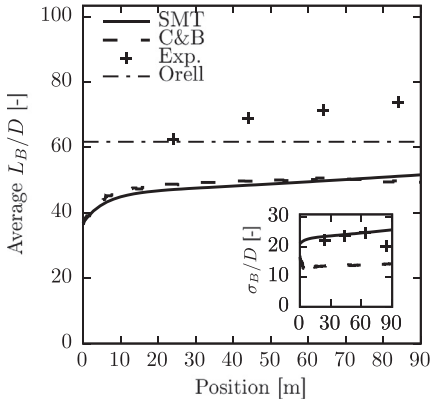

Fig. 12. Predictions of L_B/D for the experiment of Grenier (1997), with U_{SL} = 0.5 ms^{-1}, U_{SG} = 1.0 ms^{-1}. The inset figure shows the behavior of the standard deviation against position.

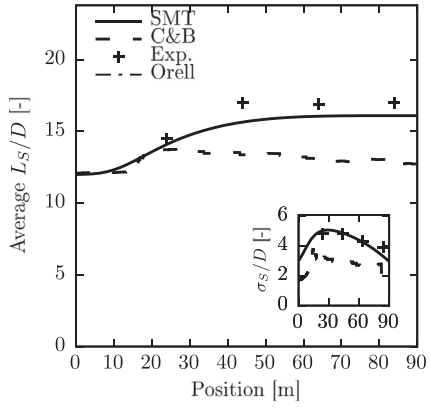

Fig. 13. Predictions of L_S/D for the experiment of Grenier (1997), with U_{SL} = 1.1 ms^{-1}, U_{SG} = 1.0 ms^{-1}. The inset figure shows the behavior of the standard deviation against position.

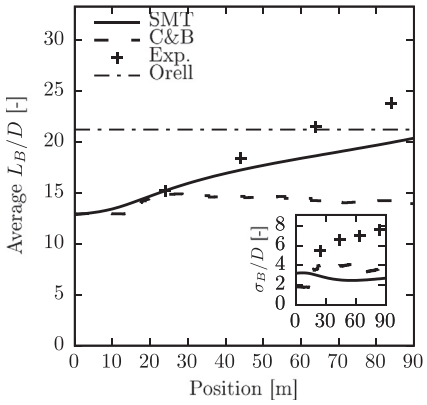

Fig. 14. Predictions of L_B/D for the experiment of Grenier (1997), with U_{SL} = 1.1 ms^{-1}, U_{SG} = 1.0 ms^{-1}. The inset figure shows the behavior of the standard deviation against position.

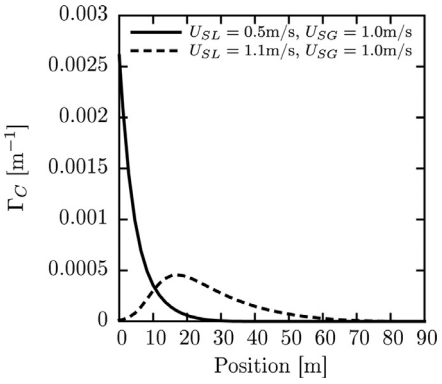

Fig. 15. Coalescence rate obtained with the SMT model for the experiments of Grenier (1997).

U_{SL} (= 0.5 ms^{-1}), the average length of the bubbles, L_B, is under predicted by 28% by the SMT model. For the higher value of 1.1 ms^{-1}, the SMT prediction is very good for most of the pipe length, with a maximum error of 25% at the 90 m position. The ST model does not predict well $\overline{L_B}$, a parameter for which the unit cell model furnishes acceptable predictions.

The success in well estimating the experimental data of $\overline{L_S}$ results from the coalescence relations that are used, which were, in any case, derived directly from the same data they are expected to predict.

The SMT model also furnishes the coalescence rate for each pipe position. Fig. 15 shows that, for the studied cases, the coalescence process ceases at about 30 m from the pipe inlet. This result suggests that the coalescence process is responsible for the flow insensitivity on the initial conditions far from the mixing point.

Figs. 16–18 show a comparison between the measured and predicted distributions for the experiments of Cook and Behnia (2000). For better comparison with the original work, the number of cells tracked in the ST model was set to 500. The unit cell model predictions are illustrated by the vertical lines. Predictions obtained with application of the SMT and ST models are good. The slug capturing method did not perform well for the shown conditions.

The mean and standard deviation values of L_s/D in Figs. 16 through 18 are shown in Table 3. The differences between predictions obtained through both methods are small and the agreement with the experiments is good. The SMT apparently better predicts the standard deviation, but discrepancies are normally below 25%.

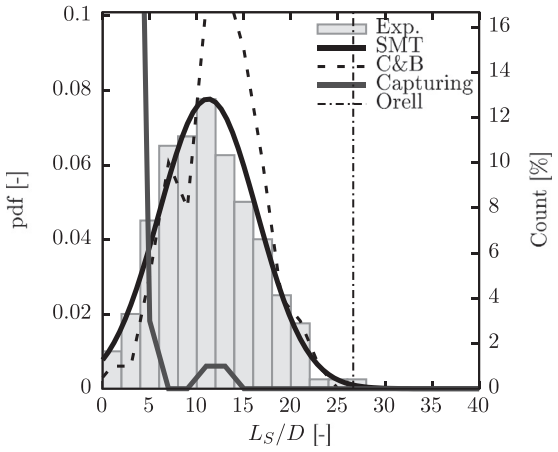

Fig. 16. Predictions of distributions of L_S/D, at 10-m, for the experiment of Cook and Behnia (2000), with $U_{SL} = 0.6\,\mathrm{ms}^{-1}$, $U_{SG} = 0.6\,\mathrm{ms}^{-1}$.

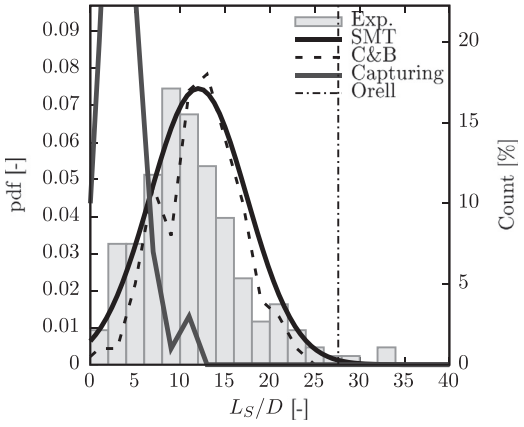

Fig. 17. Predictions of distributions of L_S/D, at 10-m, for the experiment of Cook and Behnia (2000), with $U_{SL} = 1.0\,\mathrm{ms}^{-1}$, $U_{SG} = 1.5\,\mathrm{ms}^{-1}$.

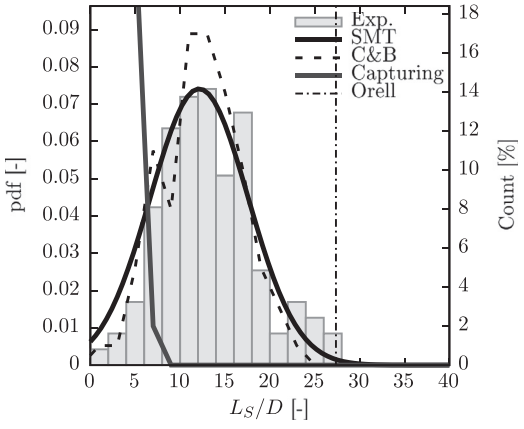

Fig. 18. Predictions of distributions of L_S/D, at 10 m, for the experiment of Cook and Behnia (2000), with $U_{SL} = 1.5\,\mathrm{ms}^{-1}$, $U_{SG} = 2.0\,\mathrm{ms}^{-1}$.

Table 3
Comparison between the data of Cook and Behnia (2000) and the ST and SMT models for predictions of L_s/D.

	Figure	Exp.	ST (C&B)	SMT
L_s/D Mean	16	11.25	12.50	11.17
	17	11.34	12.29	11.82
	18	13.32	12.50	11.91
L_s/D Std. Dev.	16	5.41	4.58	5.21
	17	5.81	4.64	5.36
	18	5.27	4.88	5.38

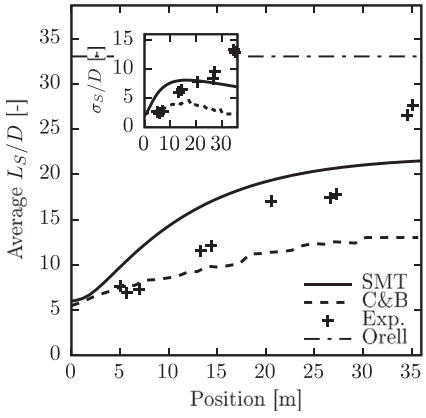

Fig. 19. Predictions of L_S/D for the experiment of Ujang et al. (2006), with $U_{SL} = 0.41\,\mathrm{ms}^{-1}$, $U_{SG} = 2.36\,\mathrm{ms}^{-1}$. The inset figure shows the behavior of the standard deviation against position.

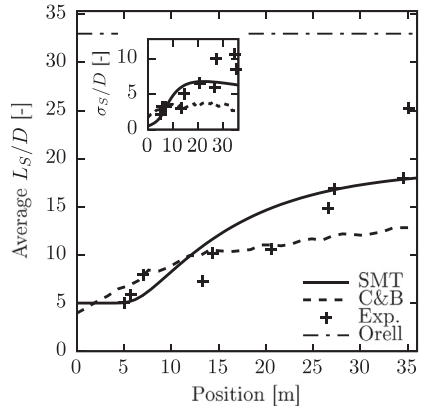

Fig. 20. Predictions of L_S/D for the experiment of Ujang et al. (2006), with $U_{SL} = 0.61\,\mathrm{ms}^{-1}$, $U_{SG} = 2.55\,\mathrm{ms}^{-1}$. The inset figure shows the behavior of the standard deviation against position.

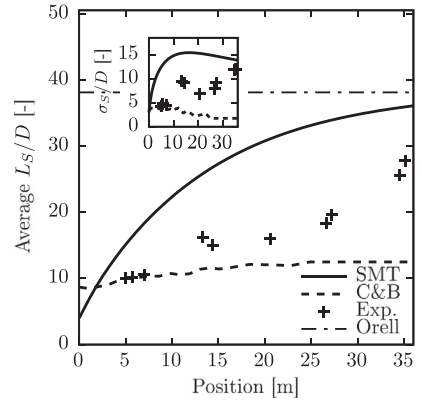

Fig. 21. Predictions of L_S/D for the experiment of Ujang et al. (2006), with $U_{SL} = 0.61\,\mathrm{ms}^{-1}$, $U_{SG} = 4.64\,\mathrm{ms}^{-1}$. The inset figure shows the behavior of the standard deviation against position.

A comparison between the experimental data of Ujang et al. (2006) and the present numerical estimations is shown in Figs. 19–21. Results provided by the SMT model are clearly better than those obtained through the ST model. In the computations, no model constant has been particularly fixed; constants attain the same values that were considered in the previous simulations and that took as reference the experiments of Grenier (1997).

Figs. 22–24 show the slug length distributions obtained at 13.32, 20.57 and 34.55 m, respectively, for the conditions

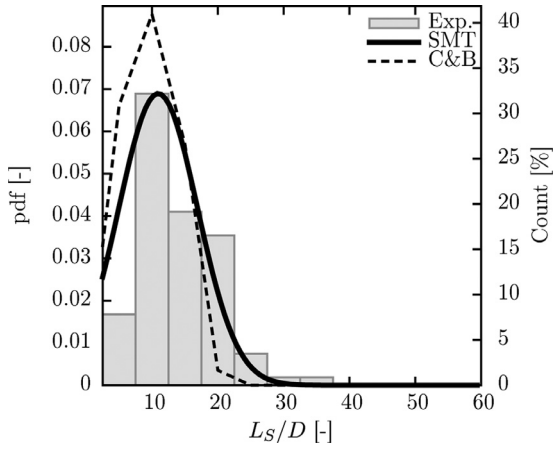

Fig. 22. Predictions of distributions of L_S/D, at 13.32 m, for the experiment of Ujang et al. (2006), with $U_{SL} = 0.61\,\mathrm{ms}^{-1}$, $U_{SG} = 2.55\,\mathrm{ms}^{-1}$.

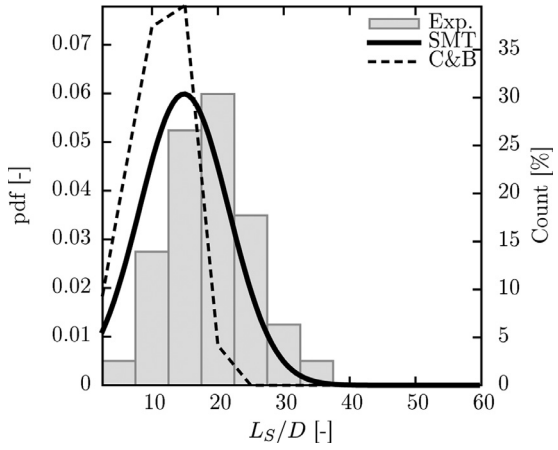

Fig. 23. Predictions of distributions of L_S/D, at 20.57 m, for the experiment of Ujang et al. (2006), $U_{SL} = 0.61\,\mathrm{ms}^{-1}$, $U_{SG} = 2.55\,\mathrm{ms}^{-1}$.

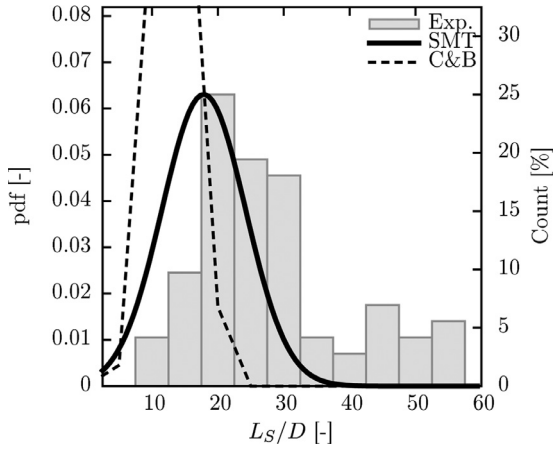

Fig. 24. Predictions of distributions of L_S/D, at 34.55 m, for the experiment of Ujang et al. (2006), $U_{SL} = 0.61\,\mathrm{ms}^{-1}$, $U_{SG} = 2.55\,\mathrm{ms}^{-1}$.

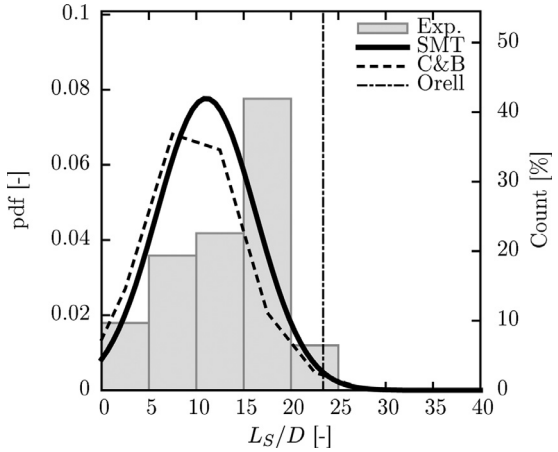

Fig. 25. Predictions of distributions of L_S/D, at 9 m, for the experiment of Gonçalves et al. (2018), $U_{SL} = 0.72\,\mathrm{ms}^{-1}$, $U_{SG} = 0.27\,\mathrm{ms}^{-1}$.

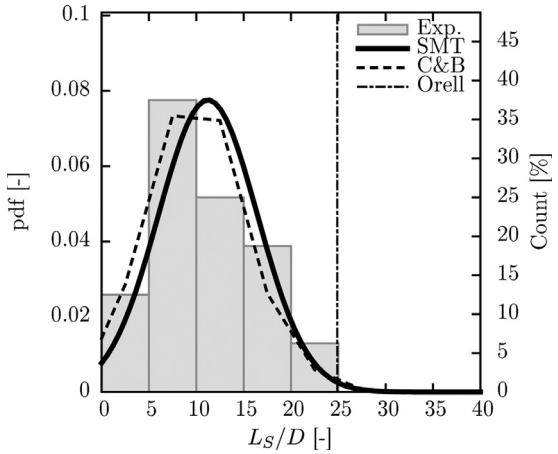

Fig. 26. Predictions of distributions of L_S/D, at 9 m, for the experiment of Gonçalves et al. (2018), $U_{SL} = 0.72\,\mathrm{ms}^{-1}$, $U_{SG} = 0.5\,\mathrm{ms}^{-1}$.

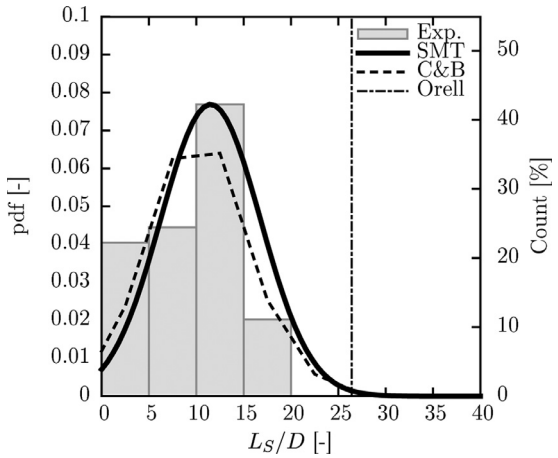

Fig. 27. Predictions of distributions of L_S/D, at 9 m, for the experiment of Gonçalves et al. (2018), $U_{SL} = 0.72\,\mathrm{ms}^{-1}$, $U_{SG} = 0.78\,\mathrm{ms}^{-1}$.

$U_{SL} = 0.61\,\mathrm{ms}^{-1}$ and $U_{SG} = 2.55\,\mathrm{ms}^{-1}$. At the first station, results provided by the SMT and ST are comparable and very close to the experiments. However, as the bubbles move downstream, the computations tend to underestimate the mean length of the bubbles. At position $x = 34.55$ m the ST prediction is poor.

The slug length distributions described in Gonçalves et al. (2018) are shown in Figs. 25–33. All mean length distributions were obtained at the same position (9 m downstream of the gas injection point) for nine different experimental conditions (combinations of U_{SL} and U_{SG}). For the lowest U_{SL} ($= 0.72\,\mathrm{ms}^{-1}$), the agreement between computations and experiments is very good. As U_{SL} increases, however, predictions of L_S/D tend to be overestimated by the models.

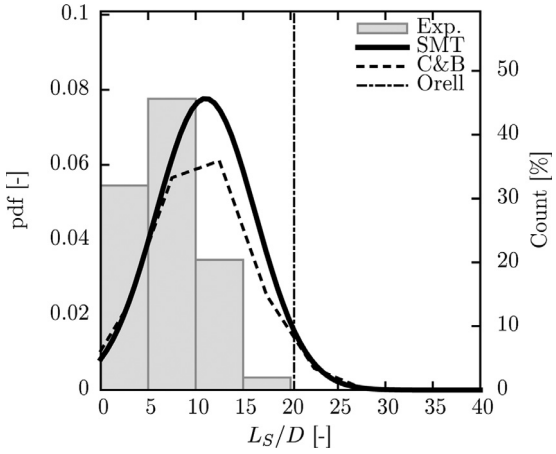

Fig. 28. Predictions of distributions of L_S/D, at 9 m, for the experiment of Gonçalves et al. (2018), $U_{SL} = 1.27\,\text{ms}^{-1}$, $U_{SG} = 0.22\,\text{ms}^{-1}$.

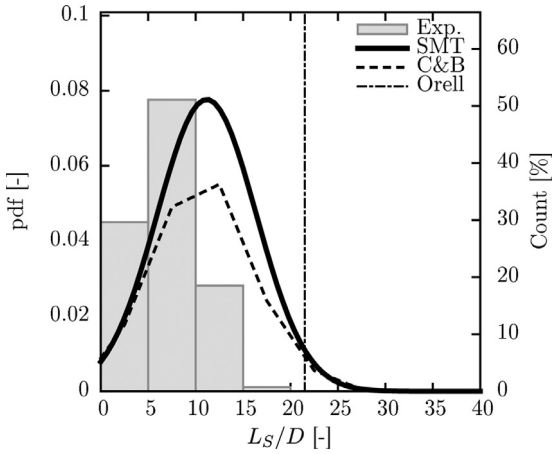

Fig. 29. Predictions of distributions of L_S/D, at 9 m, for the experiment of Gonçalves et al. (2018), $U_{SL} = 1.27\,\text{ms}^{-1}$, $U_{SG} = 0.42\,\text{ms}^{-1}$.

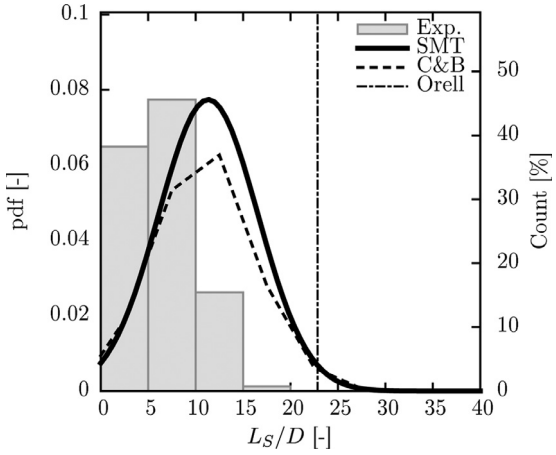

Fig. 30. Predictions of distributions of L_S/D, at 9 m, for the experiment of Gonçalves et al. (2018), $U_{SL} = 1.27\,\text{ms}^{-1}$, $U_{SG} = 0.68\,\text{ms}^{-1}$.

A comparison of the SMT model with the vertical slug flow data of Mayor et al. (2008) is presented next (Figs. 34–37). The author's predictions with an ST model (Mayor et al., 2007) are also shown. As mentioned before, in all simulations, the SMT and ST models consider a cylindrical bubble shape; the coalescence

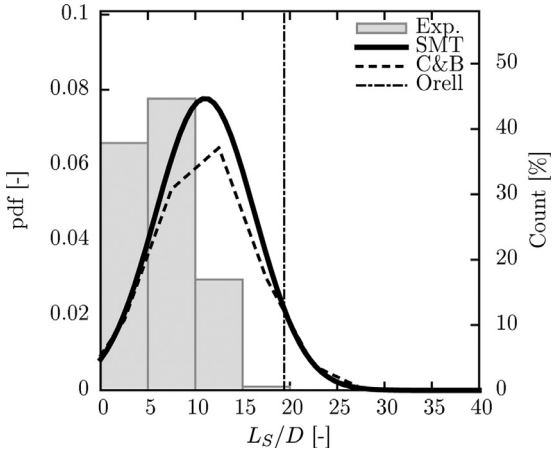

Fig. 31. Predictions of distributions of L_S/D, at 9 m, for the experiment of Gonçalves et al. (2018), $U_{SL} = 1.81\,\text{ms}^{-1}$, $U_{SG} = 0.21\,\text{ms}^{-1}$.

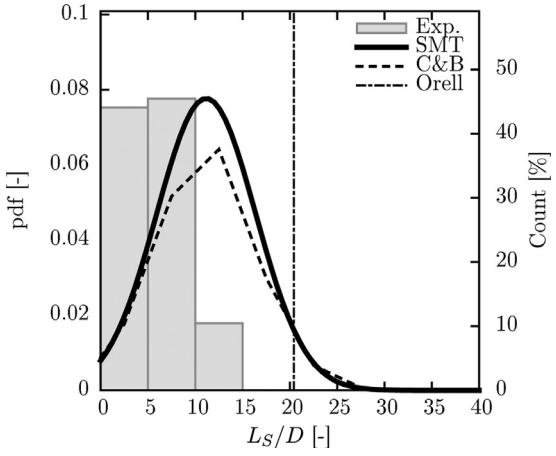

Fig. 32. Predictions of distributions of L_S/D, at 9 m, for the experiment of Gonçalves et al. (2018), with $U_{SL} = 1.81\,\text{ms}^{-1}$, $U_{SG} = 0.43\,\text{ms}^{-1}$.

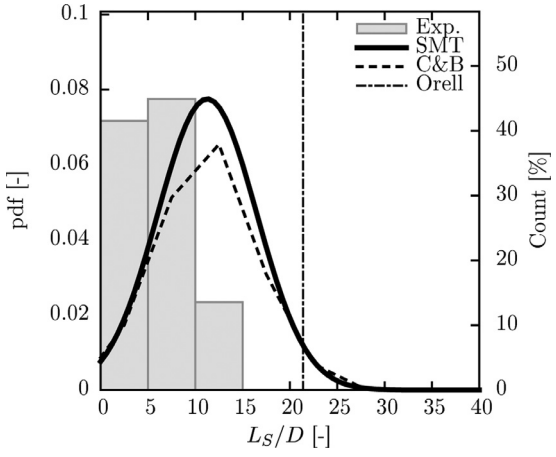

Fig. 33. Predictions of distributions of L_S/D, at 9m, for the experiment of Gonçalves et al. (2018), with $U_{SL} = 1.81\,\text{ms}^{-1}$, $U_{SG} = 0.65\,\text{ms}^{-1}$.

velocity is given by:

$$v(L_S) = 2.4e^{-0.8(L_S/D)^{0.9}} \tag{75}$$

The initial distribution of L_S considers $\overline{L_S/D} = 5$ and $\sigma_S/D = 2$.

For vertical flows in the pipe with ID = 32 mm, the overall predictions of distributions of L_S/D through the SMT and ST models are comparable to each other and tend to overestimate

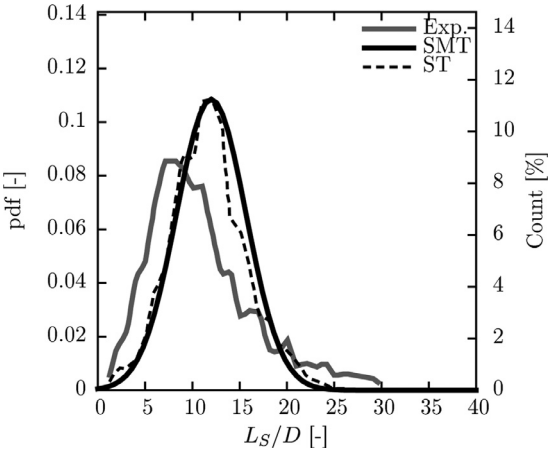

Fig. 34. Predictions of distributions of L_S/D for the experiment of Mayor et al. (2008), Conditions 1 (Table 2; $U_{LS} = 0.1\,\mathrm{ms}^{-1}$, $U_{GS} = 0.09\,\mathrm{ms}^{-1}$, $D = 32$ mm).

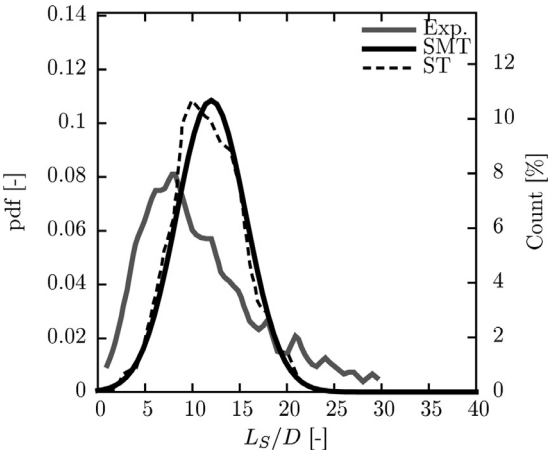

Fig. 35. Predictions of distributions of L_S/D for the experiment of Mayor et al. (2008), Conditions 2 (Table 2; $U_{LS} = 0.1\,\mathrm{ms}^{-1}$, $U_{GS} = 0.26\,\mathrm{ms}^{-1}$, $D = 32$ mm).

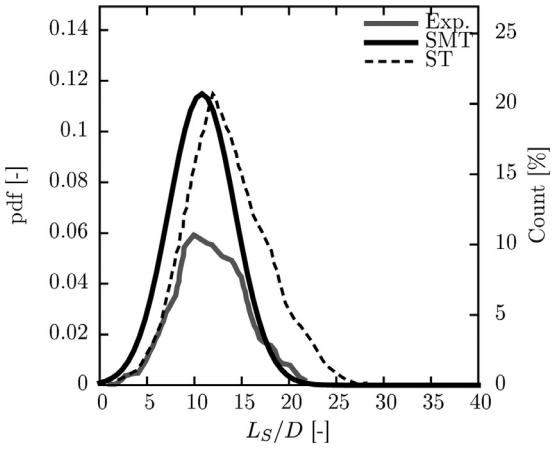

Fig. 36. Predictions of distributions of L_S/D for the experiment of Mayor et al. (2008), Conditions 3 (Table 2; $U_{LS} = 0.07\,\mathrm{ms}^{-1}$, $U_{GS} = 0.10\,\mathrm{ms}^{-1}$, $D = 52$ mm).

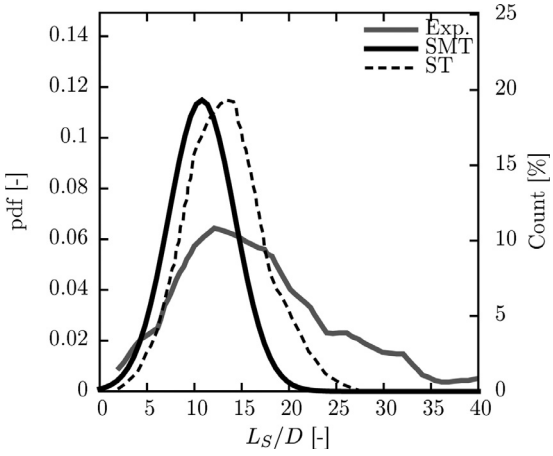

Fig. 37. Predictions of distributions of L_S/D for the experiment of Mayor et al. (2008), Conditions 4 (Table 2; $U_{LS} = 0.1\,\mathrm{ms}^{-1}$, $U_{GS} = 0.21\,\mathrm{ms}^{-1}$, $D = 52$ mm).

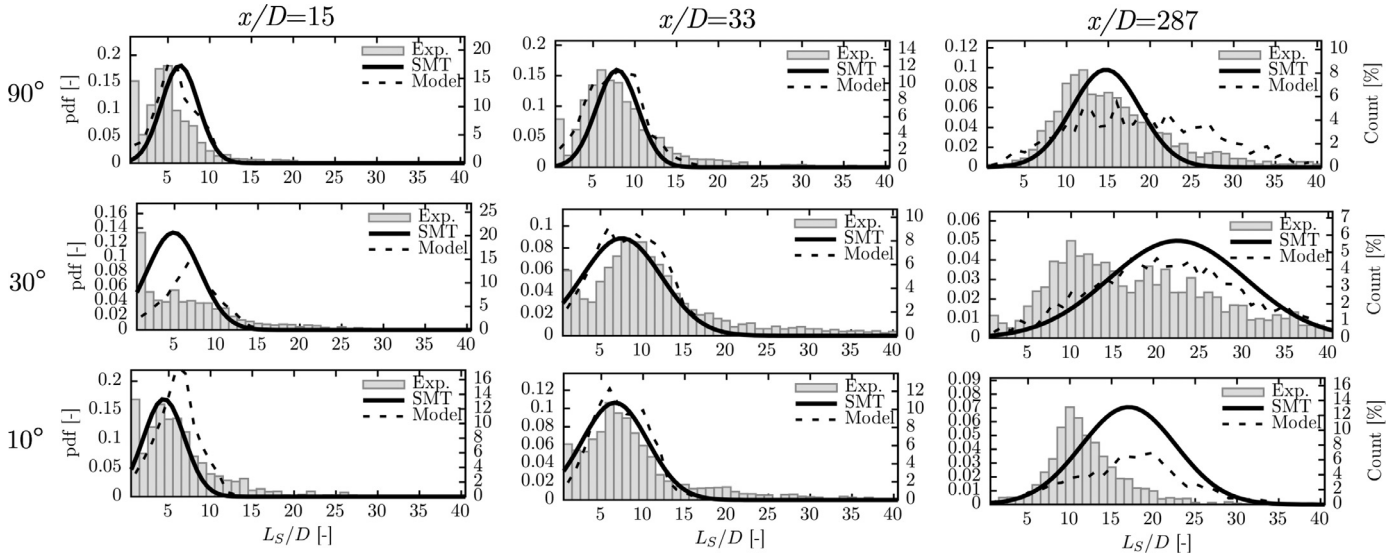

Fig. 38. Predictions of distributions of L_S/D, at several positions and inclinations, for the data of van Hout et al. (2003), with $U_{SL} = 0.01\,\mathrm{ms}^{-1}$, $U_{SG} = 0.41\,\mathrm{ms}^{-1}$, $D = 24$ mm. The results predicted by van Hout et al. (2003) are shown through dashed lines.

the experimental mean. For the 52 mm ID pipe, however, the ST model yields sightly larger values of L_S as compared to the SMT. Both models predict relatively well the experimental data.

Fig. 38 presents a comparison between the measured and predicted data of van Hout et al. (2003), together with predictions obtained through the SMT model. The inclination-dependent velocity expressions proposed by the original authors were used for the current simulations.

The SMT seems to perform as well, or better, than the tracking method in most conditions. The largest discrepancies can be noticed in the inclinations of 30 and 10 degrees, especially for the station farthest downstream. In these conditions, both theoretical predictions seem to overestimate the lengths of the long slugs. Neither model is capable of predicting well the large number of very short slugs near the inlet.

7. Final remarks

An alternative model to predict the slug flow structure is proposed, based on the transport of the statistical moments along the pipe. A set of five simple equations was developed and it was shown that they are capable of describing the flow structure at any position of the pipe with the same accuracy of the slug-tracking model. The present approach has the advantage of a better comprehension of the process because it expresses the influence of every relevant phenomenon – slug formation, interaction between bubbles, gas expansion and bubbles coalescence – on the structure evolution. A comparison between the SMT model and twenty four distinct experimental data sets has shown the model to perform very well. Furthermore, the SMT model offers an extreme economy in the simulation time. Fig. 10 shows that even for relatively short pipes (64 m) a gain of two orders of magnitude is obtained in computing time as compared to slug-tracking models. The work has also shown that an interaction law, derived from experiments that investigate controlled isolated pairs of bubbles, allows the ST and SMT models to predict well the evolution of slug flows.

Acknowledgments

JRFN is grateful to professor Jean Fabre for his seminal ideas, encouragement and permanent support on the development of the SMT model. Many of the underlying concepts here presented have stemmed from his firm belief that slug flow is a problem prone to statistical description.

The authors are grateful to Dr. Hamidreza Anbarlooei for the data shown regarding the slug capturing method. APSF is grateful to the Brazilian National Research Council (CNPq) for the award of a Research Fellowship (No 305338/2014-5). The work was partially supported by the Rio de Janeiro Research Foundation (FAPERJ) through Grant E-26/202.912/2015.

References

Bandeira, F.J.S., Gonçalves, G.F.N., Loureiro, J.B.R., Silva Freire, A.P., 2017. Turbulence and bubble break up in slug flow with wall injection. Flow, Turbul. Combust. 98, 923–945.

Barnea, D., Taitel, Y., 1993. A model for slug length distribution in gas-liquid slug flow. Int. J. Multiph. Flow 19 (5), 829–838.

Bendiksen, K.H., 1984. An experimental investigation of the motion of long bubbles in inclined tubes. Int. J. Multiph. Flow 10 (4), 467–483.

Cook, M., Behnia, M., 2000. Slug length prediction in near horizontal gas-liquid intermittent flow. Chem. Eng. Sci. 55 (11), 2009–2018.

Dhulesia, H., Bernicot, M., Deheuvels, P., 1991. Statistical analysis and modelling of slug lengths. In: Proceedings of the BHRG 5th International Conference On Multiphase Production, pp. 80–112.

Dukler, A.E., Hubbard, M.G., 1975. A model for gas-liquid slug flow in horizontal and near horizontal tubes. Ind. Eng. Chem. Fund. 14 (4), 337–347.

Evje, S., Flåtten, T., 2003. Hybrid flux-splitting schemes for a common two-fluid model. J. Comput. Phys. 192 (1), 175–210.

Fabre, J., Liné, A., 1992. Modeling of two-phase slug flow. Ann. Rev. Fluid Mech. 24 (1), 21–46.

Fabre, J., Line, A., Peresson, L., 1989. Two-fluid/two-flow-pattern model for transient gas-liquid flow in pipes. In: Proceedings of the 4th International Conference Multiphase Flow, pp. 19–21.

Fagundes Netto, J.R., 1999. Dynamique de poches de gaz isollees en ecoulement permanent et non permanent horizontal. Institut National Polytechnique de Toulouse.

Fagundes Netto, J.R., Fabre, J., Peresson, L., 2001. Bubble-bubble interaction in horizontal two-phase slug flow. J. Braz. Soc. Mech. Sci. 23.

Gonçalves, G.F.N., Baungartner, R., Loureiro, J.B.R., Silva Freire, A.P., 2018. Slug flow models: feasible domain and sensitivity to input distributions. J. Petrol. Sci. Eng. 169 (May), 705–724.

Grenier, P., 1997. Evolution des longueurs de bouchons en ecoulement intermittent horizontal. Institut National Polytechnique de Toulouse.

Issa, R.I., Kempf, M.H.W., 2003. Simulation of slug flow in horizontal and nearly horizontal pipes with the two-fluid model. Int. J. Multiph. Flow 29, 69–95.

Mayor, T.S., Ferreira, V., Pinto, A.M.F.R., Campos, J.B.L.M., 2008. Hydrodynamics of gas-liquid slug flow along vertical pipes in turbulent regime-An experimental study. Int. J. Heat Fluid Flow 29 (4), 1039–1053. doi:10.1016/j.ijheatfluidflow.2008.02.013.

Mayor, T.S., Pinto, A.M.F.R., Campos, J.B.L.M., 2007. Hydrodynamics of gas-Liquid slug flow along vertical pipes in turbulent regime: A Simulation study. Chem. Eng. Res. Des. 85 (11), 1497–1513. doi:10.1205/cherd06245.

Moissis, R., Griffith, P., 1962. Entrance effects in a two-phase slug flow. J. Heat Trans. 29–39.

Moissis, R., Griffith, P., 1981. Drift in horizontal two-phase flow in horizontal pipes. Can. J. Chem. Eng. 398–399.

Nicklin, D., Wilkes, J., Davidson, J., 1962. Two-phase flow in vertical tubes. Trans. Inst. Chem. Eng 40, 61–68.

Nieckele, A.O., Carneiro, J.N.E., Chucuya, R.C., Azevedo, J.H.P., 2013. Initiation and statistical evolution of horizontal slug flow with a two-Fluid model. J. Fluids Eng. 135 (12), 121302.

Nydal, O.J., 2012. Dynamic Models in Multiphase Flow. Energy Fuels.

Nydal, O.J., Banerjee, S., 1996. Dynamic slug tracking simulations for gas-Liquid flow in pipelines. Chem. Eng. Commun. 141–142 (November 2014), 13–39.

Nydal, O.J., Pintus, S., Andreussi, P., 1992. Statistical characterization of slug flow in horizontal pipes. Int. J. Multiph. Flow 18 (3), 439–453.

Orell, A., 2005. Experimental validation of a simple model for gas-liquid slug flow in horizontal pipes. Chem. Eng. Sci. 60 (5), 1371–1381.

Schulkes, R., 2011. Slug frequencies revisited. Proceedings of the 15th International Conference on Multiphase Production Technology (1969), 311–325.

Spedding, P.L., Hand, N.P., 1997. Prediction in stratified gas-liquid co-current flow in horizontal pipelines. Int. J. Heat Mass Trans. 40 (8), 1923–1935.

Straume, T., Nordsven, M., Bendiksen, K., 1992. Numerical simulation of slugging in pipelines. Multiph. Flow Wells Pipel. ASME 144, 3–112.

Taitel, Y., Barnea, D., Dukler, A., 1980. Modelling flow pattern transitions for steady upward gas-liquid flow in vertical tubes. AIChE J. 26, 345–354.

Taitel, Y., Dukler, A., 1976. A model for predicting flow regime transitions in horizontal and near horizontal gas-Liquid flow. AIChE J. 22 (1), 47–55.

Ujang, P.M., Lawrence, C.J., Hale, C.P., Hewitt, G.F., 2006. Slug initiation and evolution in two-phase horizontal flow. Int. J. Multiph. Flow 32 (5), 527–552.

van Hout, R., Shemer, L., Barnea, D., 2003. Evolution of hydrodynamic and statistical parameters of gas-liquid slug flow along inclined pipes. Chem. Eng. Sci. 58, 115–133.

Wallis, G.B., 1969. One-Dimensional Two-phase Flow. McGraw-Hill, New York.